Exciton Relaxation in PbSe Nanorods

Jun Yang,[†,*] Byung-Ryool Hyun,[†] Anthony J. Basile,[‡] and Frank W. Wise[†,*]

[†]School of Applied and Engineering Physics, Cornell University, Ithaca, New York, 14850, United States and [‡]Department of Materials Science and Engineering, Cornell University, Ithaca, New York, 14850, United States

ABSTRACT

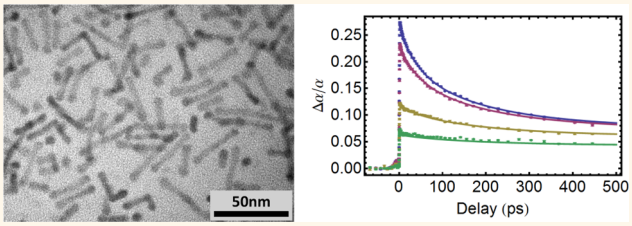

Measurements of the picosecond-time-scale dynamics of photoexcited electrons in PbSe nanorods are reported. The intraband ($1\Pi \rightarrow 1\Sigma$) relaxation occurs with a time constant of ~500 fs, which corresponds to a fast energy-relaxation rate of ~0.6 eV/ps. The biexciton lifetime in PbSe nanorods is significantly (3–4 times) longer than the lifetime of PbSe quantum dots with the same energy gap, roughly as expected considering the increased volume. The multiexciton lifetimes of PbSe nanorods scale as expected for a bimolecular recombination mechanism. Implications of the observed relaxations will be discussed.

KEYWORDS: nanorod · PbSe · 1D · Auger recombination · intraband relaxation · exciton · biexciton

Lead-salt (PbS, PbSe, and PbTe) nanostructures currently attract much interest. Due to the large dielectric constants and small carrier masses of the parent crystals, their exciton Bohr radii are large, 20–46 nm. Nanocrystals that strongly confine charge carriers are easily synthesized by colloidal chemistry. Moreover, their nearly symmetric conduction and valence bands lead to relatively simple electronic structure, compared to II–VI, III–V, and column-IV materials. By changing the size of PbS or PbSe quantum dots, their absorption and emission peaks can be tuned across the near-infrared spectrum, which makes them strong candidates for the active material in solar energy applications. Solar cells made with PbS or PbSe quantum dots as the active material have recently achieved 6% power-conversion efficiency.[1]

In the past decade, research on quasi-one-dimensional (1D) nanostructures has grown substantially. A number of overviews of nanowire (NW) and nanorod (NR) research have been published.[2–4] In a 1D structure the Coulomb interaction can act primarily through the host medium, so it will not be screened as effectively as in 0D (quantum dot) or 3D (bulk) materials. Thus, the transition from the limit of strong confinement to the limit of strong correlation can be investigated as the length of the nanostructure changes.

Coulomb interactions are manifested dramatically in carrier dynamics, as Auger processes are critically important in nanostructures.[5,6] They present a major impediment to creation of optical gain[7,8] and are directly relevant to multiple-exciton generation (MEG).[9] Several studies of ultrafast electron dynamics in 1D or quasi-1D quantum-confined materials have been reported. For example, in small aspect ratio CdSe NRs, relaxation of higher energy state is faster, while the lowest energy state population rises slower compared with QDs of same band-gap energy.[10] This was explained as due to the reduced energy level degeneracy caused by the shape anisotropy. In NRs with larger aspect ratio, carrier thermalization happens in a dense manifold of high-energy states, and the behavior is similar to the bulk material.[11] CdSe NRs with different diameters but similar lengths were studied, and intraband relaxation was found to be faster in smaller rods,[12] which is consistent with hole-assisted Auger relaxation. Multiexciton relaxation has been studied in CdSe NRs[13] and single-walled carbon nanotubes.[14] The relaxation was explained as a bimolecular Auger recombination in these 1D materials, in contrast to the three-body Auger relaxation found in quantum dots[15] and bulk materials.

There are few reports of anisotropic lead-salt nanostructures, mostly due to the difficulty of synthesizing anisotropic particles with isotropic (rock salt) crystal structure. Koh *et al.* recently reported a one-pot, catalyst-free synthesis of PbSe NRs with high optical quality.[16] The structures have diameters around 4 nm and are 20–30 nm long, so both dimensions are small compared to the exciton Bohr radius. A four-band envelope-function calculation[17,18] accounts well for the observed optical transitions. An important prediction of

* Address correspondence to jy449@cornell.edu; frank.wise@cornell.edu.

Received for review June 20, 2012 and accepted August 5, 2012.

Published online August 05, 2012
10.1021/nn302739e

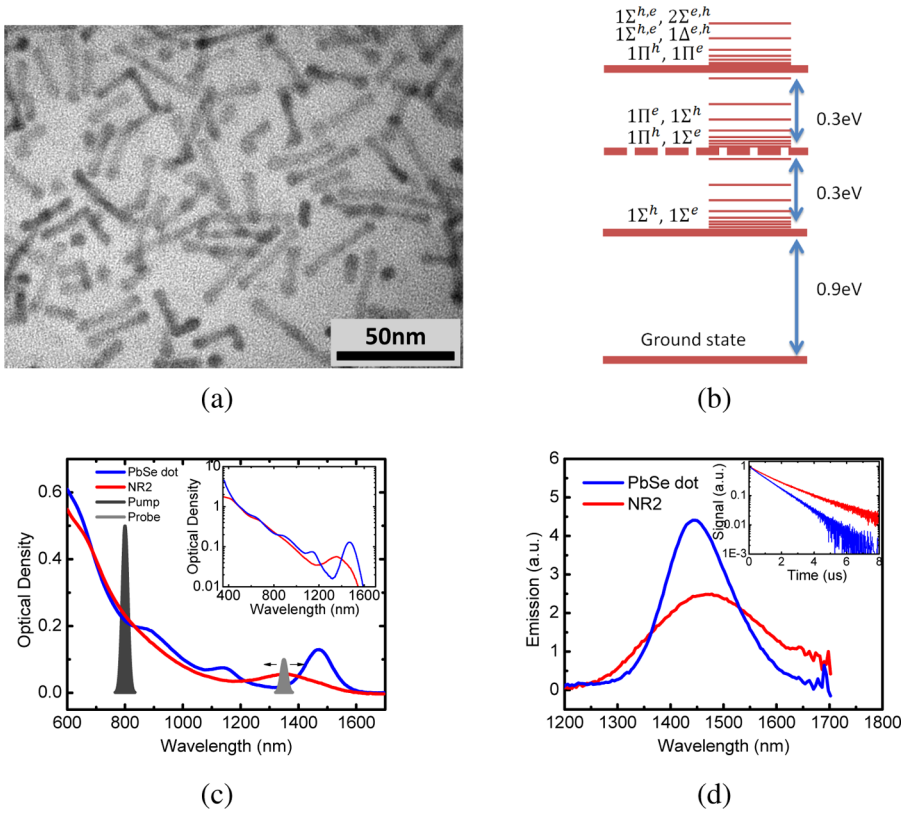

Figure 1. Structural and optical characterization of samples. (a) TEM image of nanorod sample NR2, which has dimensions 4.5 ± 0.6 nm $\times$ 28 ± 7 nm. (b) Theoretical energy spectrum of sample NR2. Here $1\Pi-1\Sigma$ states are dashed, as the $1\Sigma-1\Pi$ transition is optically forbidden. (c) Absorption spectrum of NR2 and a PbSe dot sample for comparison. Pump (800 nm) and probe wavelengths (spanning from the blue side to the red side of the absorption peak) are shown. Inset: Absorption spectra on semilogarithmic scale, to show features at the high-energy side. (d) Emission spectrum of NR2 and PbSe dot sample. Inset: Fluorescence decays.

the theory is that the electrons and holes exist as tightly bound excitons in PbSe NRs, in contrast to the situation in lead-salt quantum dots.[19] In terms of electron relaxation in 1D lead-salt structures, a theoretical treatment concludes that Auger recombination is forbidden for the lowest biexciton state.[20] On the other hand, Cunningham *et al*. reported that the efficiency of MEG in quasi-1D PbSe structures is significantly higher than that of PbSe quantum dots, and the MEG energy threshold is much lower.[21] This observation implies significant potential for NR solar cells and increases the motivation to study carrier dynamics in lead-salt NRs.

Here, we report femtosecond optical studies of the relaxation of excitons in PbSe nanorods with dimensions near 4 nm $\times$ 20 nm. Excitons created in excited 1Π states relax to the lowest exciton state in two stages in the first few picoseconds. The fast energy relaxation rate is similar to that found in PbSe quantum dots. Multiple excitons decay on the 100 ps time scale. The biexciton lifetime is found to be several times larger than that of quantum dots with the same energy gap, roughly as expected based on the volumes of the structures. However, the multiexciton lifetimes scale as expected for a bimolecular recombination process, which is expected for tightly bound excitons.

We synthesized PbSe NRs using the one-pot reaction developed previously.[16] A typical transmission electron microscope (TEM) image is shown in Figure 1a. High-resolution TEM images (Supporting Information) confirm that the NRs are single-crystalline and grow along the (100) direction. We studied six NR samples (which we refer to as NR1 to NR6), with diameters ranging from 3.3 to 4.5 nm and lengths from 20 to 30 nm. These have lowest exciton transitions between 1100 and 1430 nm. It was difficult for us to grow high-quality NRs outside these ranges. Within each sample, there is about 10% variation in diameter and 25% in length. A PbSe quantum dot sample with lowest exciton transition near 1470 nm was also studied for comparison.

The theoretical exciton spectrum of a 4.5 nm $\times$ 28 nm PbSe NR is shown in Figure 1b. The single particle states are labeled as follows: $kX^{e,h}_{|n|}$ for the kth electron or hole level, with z component of total angular momentum equal to n and angular momentum projection of the conduction (valence) band component of the wave function equal to $|m| = 0, 1, 2, \ldots$ for $X = \Sigma, \Pi, \Delta, \ldots$.[17] Due to strong electron–hole interaction, we draw the energy levels in terms of exciton states instead of single-particle states. A typical absorption spectrum is shown in Figure 1c along with the spectrum of the PbSe quantum dot sample for reference. The corresponding fluorescence spectra and decays are shown in Figure 1d. The fluorescence lifetime of the NRs is 1.7 μs.

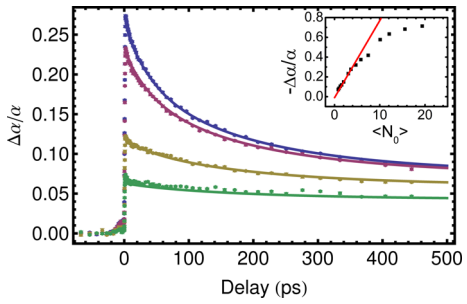

Figure 2. Saturated absorption traces for pump fluences corresponding to $\langle N_0 \rangle$ = 0.84, 1.6, 3.1, and 3.6, from bottom to top. α is the optical density at the probe wavelength, measured with the CW spectrometer, and $\Delta\alpha$ is the change in optical density due to the pump pulse. Solid lines are multiexponential fits (see text), with τ_2 = 217 ps, τ_3 = 65 ps. Inset: Signal magnitude measured at t = 3 ps after the initial excitation *versus* initial excitation ($\langle N_0 \rangle$). The line is the fit for low excitation.

RESULTS

Important relaxation processes occur on the 100 ps and 1 ps time scales and were studied using standard time-resolved transient absorption measurements. We will begin with an overview of the experimental data and discussion of the dynamics on the ~100 ps scale, which provide information on Auger relaxation of multiple ground-state excitons. Then, we will focus on the ~1 ps time scale, which corresponds to energy relaxation within the electron or hole states. Qualitatively similar results were obtained for all samples. Results obtained with sample NR2 (4.5 ± 0.6 nm × 28 ± 7 nm) will be discussed in detail, and then results obtained from all the samples will be summarized.

Multiexciton Dynamics. The saturated-absorption traces obtained by excitation at 800 nm and probing the lowest exciton transition (Figure 2) exhibit features that are familiar from work on quantum dots[22−24] and are qualitatively similar to data presented in the study of MEG in 1D structures.[21] With initial excitation $\langle N_0 \rangle$ below one electron−hole pair per NR, the trace shows negligible change on the time scale of the measurement (500 ps), as expected from the microsecond population decay observed in fluorescence. As the pump fluence increases, faster decay components appear progressively, which correspond to discrete multiexciton relaxation due to Auger recombination.

Modeling of the exciton dynamics follows the approach used for quantum dots.[15,22] Since the excitons are created by photons with energy lower than twice the energy gap, MEG does not occur, and the excitation probability satisfies the Poisson distribution: the probability that a NR has n excitons at t = 0 is

$$P_n(t = 0) = \frac{\langle N_0 \rangle^n}{n!} e^{-\langle N_0 \rangle} \quad (1)$$

The excitons decay to the lowest state within a few picoseconds (this will be shown in the next section). From that point on, the exciton population distribution follows a cascade model:

$$\frac{dP_n(t)}{dt} = -\frac{P_n(t)}{\tau_n} + \frac{P_{n+1}(t)}{\tau_{n+1}} \quad (2)$$

$$\langle N(t) \rangle = \sum_{n=1} nP_n(t) \quad (3)$$

where τ_n is the n-exciton lifetime. The initial average population can be calculated as $\langle N_0 \rangle = j_p\sigma$, where j_p is the pump fluence per pulse, and σ is the absorption cross-section at the excitation wavelength. We calculated σ following previous work on PbSe quantum dots,[25] assuming that at high energy (3.1 eV) NRs and quantum dots both behave like bulk material and thus have the same cross-section per unit volume. By scaling from the measured absorption at 400 and 800 nm, we obtained the cross-section at 800 nm, the excitation wavelength. Experimentally, the absorption spectra of the NRs and quantum dots do not match exactly at high energy (Figure 1c, inset), and this introduces uncertainty into our modeling. To reflect this, along with uncertainty in measurements of the pulse fluence, we treated the cross-section as a fitting parameter. The best-fit value of this parameter was always within 25% of the nominal cross-section, which indicates that the original assumption is reasonable. The effect of inhomogeneous excitation across the sample due to absorption was also considered in the model (see Supporting Information). The saturated absorption signal 3 ps after the pump pulse varies linearly with excitation intensity up to $\langle N_0 \rangle \approx 5$ (inset of Figure 2), as expected based on similar results obtained with quantum dots.[8,22] This enabled us to directly correlate the measured signal to the number of excitons in the NR and ensured valid analysis.

By solving eq 2 with the initial condition of eq 1, we obtain the time-dependent exciton population. The parameters in the model are the absorption cross-section and the multiexciton lifetimes τ_n (n = 1−5). In solving eq 2, higher exciton states (n > 5) were neglected, due to their short expected lifetimes and small probabilities of being excited initially.

For each sample and each probe wavelength, a global fit to the experimental data recorded for all excitation levels was performed. The best-fit curves (solid lines in Figure 2) agree well with the data. The biexciton lifetime extracted from the fit, τ_2, is 210 ± 40 ps, while the triexciton lifetime, τ_3, is 64 ± 7 ps. The uncertainties in the inferred values of τ_4 and τ_5 are large, and we do not attach significance to those lifetimes.

Previous work on Auger recombination in quantum dots found that the biexciton lifetime is proportional to volume.[26] A study of CdSe NRs similarly found that the biexciton lifetime is linearly proportional to the NR length, for fixed diameter.[13] However, the lifetime is smaller than that of a quantum dot with the same volume. The biexciton lifetimes of our samples are summarized in Figure 3. The large variations in the

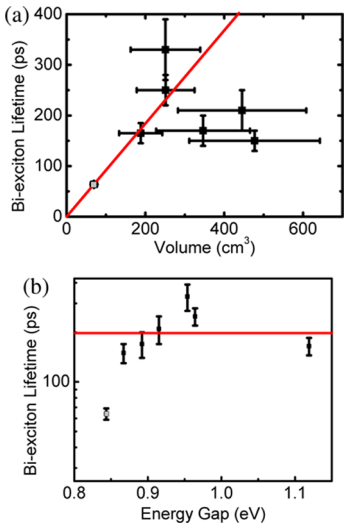

Figure 3. Biexciton lifetimes. (a) Biexciton lifetime *vs* volume. (b) Biexciton lifetime *vs* band gap. The gray square is for the quantum dot sample; the red lines are to guide the eye.

diameter and length of our NRs translate into large uncertainties in the volume, which hinders comparison to the trends observed in the prior work. We do not find systematic variation of the lifetime with volume nor with energy gap. On the other hand, the biexciton lifetimes of the NRs are 3 to 4 times longer than those of the quantum dot sample with similar energy gap, which is roughly expected based on the volume of the structures. This contrasts with the results of Cunningham *et al.*,[21] who found similar biexciton lifetimes in quantum dots and 1D structures.

The ratio of multiexciton lifetimes can shed light on the nature of the charge-carrier states in nanostructures. For a nanocrystal with N electrons and N holes (independent charges model), $\tau_N^{-1} \propto N^2(N-1)$. The scaling factor is the product of the number of all possible conduction-to-valence band transitions (N^2) and the number of carriers that can accept the extra energy ($N-1$). In this case, $\tau_2/\tau_3 = 4.5$, which was confirmed in a study of PbSe quantum dots.[15] If the electron and hole are highly correlated and form an exciton, the relaxation should be bimolecular, and the lifetimes should scale as ${\tau_N}^{-1} \propto N(N-1)$, in which case $\tau_2/\tau_3 = 3$. However, measurements of CdSe NRs[13] and carbon nanotubes[14] both found $\tau_2/\tau_3 = 1.5$. The results were explained as bimolecular recombination, but the analysis was not carried out in the small-N limit (N = 2−3). The different scaling law could be a consequence of specific band structure. For example, the small degeneracy of lowest exciton states in CdSe could result in triexcitons that contain carriers in states of other symmetries. In this case, the triexciton lifetime is likely to be longer, due to reduced probability of interband transitions of states with different symmetries. This would reduce the ratio τ_2/τ_3.[15]

Bartnik's theory predicts that the electron and hole form tightly bound excitons in PbSe NRs,[17] so bimolecular scaling would be expected. We find $\tau_2/\tau_3 = 3.3 \pm 0.3$, in good agreement with the bimolecular model of multiexciton recombination. The aspect ratios of our samples range from 5 to 7. In the case of CdSe NRs,[13] the transition from 0D to 1D corresponds to an aspect ratio of 8. However, lead-salt materials may well have a different threshold for the transition from 0D to 1D. Experiments on PbSe NRs with a wider range of aspect ratios would be helpful for clarifying this point.

Energy Relaxation. We now turn to the first few picoseconds of the saturated-absorption traces obtained with excitation at 800 nm, which provide information about the energy relaxation of hot excitons. For a NR with lowest transition at 1350 nm, the $1\Pi^h_{3/2} \rightarrow 1\Pi^e_{1/2}$ and $1\Pi^h_{1/2} \rightarrow 1\Pi^e_{1/2}$ transitions (Figure 1b) are predicted to be near 815 nm.[17] The $1\Sigma^{he}_{1/2} \rightarrow 1\Delta^{eh}_{5/2}$, $1\Delta^{eh}_{3/2}$, $2\Sigma^{eh}_{1/2}$ transitions have approximately the same energy, but much weaker oscillator strength. Thus, excitation at 800 nm should produce only NRs with carriers in the 1Π states.

Measurements of the quantum dot sample are shown in the left panel of Figure 4 for reference, and results from the NRs are shown in the right panel. Different lines correspond to different excitation fluences. The probe wavelength is 1414 nm for the NRs, on the low-energy side of the lowest exciton transition.

The data from the quantum dots exhibit an instrument-limited rise time, as reported for previous measurements of intraband electron relaxation in PbSe quantum dots.[24] The rise of the population on the time scale of the pump pulse suggests that the pump and probe transitions have an energy level in common. The 800 nm excitation is not resonant with any particular excited states in this quantum dot. According to the four-band envelope-function calculation, a PbSe quantum dot with lowest transition at 1470 nm has $1p_h \rightarrow 1p_e$ transition near 970 nm.[19] It also has $1d_h \rightarrow 1s_e$ and $1s_h \rightarrow 1d_e$ transitions around 920 nm. Although the oscillator strengths for $s_h(d_h) \rightarrow d_e(s_e)$ transitions are small, they are closer to the excitation wavelength and thus contribute the instantaneous rising part of the transient-absorption traces. The instrument-limited rise is followed by the population increase that is attributed to the intraband relaxation in the quantum dots ($d_e \rightarrow s_e$, $d_h \rightarrow s_h$). In contrast, the signals from the NR sample exhibit only a well-resolved rise, which we attribute to population relaxing to the lowest manifolds of electron and hole states. By fitting traces from the same sample at different excitation fluences, a time constant of ~500 fs is inferred (Figure 4).

After the initial 500 fs rise, the transient-absorption traces depend on the probe wavelength (Figure 5a). On the high-energy side of the lowest transition, the signal reaches a peak at a delay near 1 ps and then decays to a lower level over the next few picoseconds. On the low-energy side of the transition, the trace continues to rise. At all probe wavelengths, a quasi-steady state is reached at ~3 ps. This indicates that the energy relaxation is a

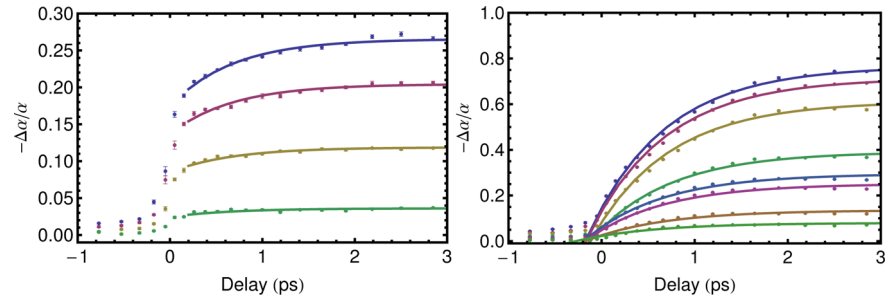

Figure 4. Rising edge of transient absorption for different pump fluence. Left: Quantum dot probed at 1470 nm, $\langle N_0 \rangle = 0.7, \ldots, 3.3$, from bottom to top. Right: NR2 probed at 1414 nm, $\langle N_0 \rangle = 0.8, \ldots, 2.5$. Due to a much larger absorption cross-section for NR, it is easier to probe higher excitation states in NR without any sign of sample damage.

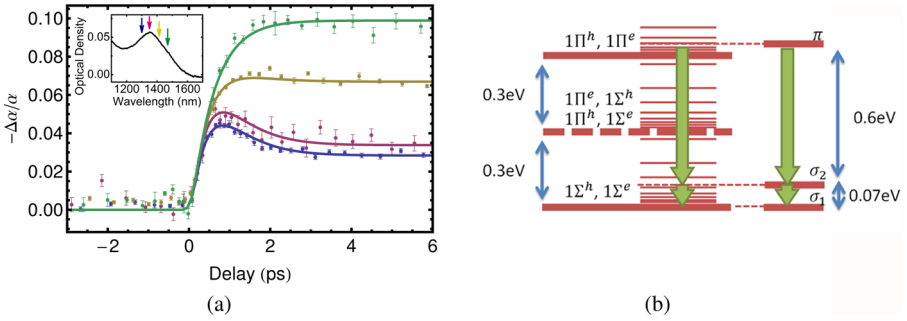

Figure 5. (a) Rising edge of transient absorption of sample NR2 at 1300, 1350, 1414, and 1470 nm. Pump wavelength 800 nm, $\langle N_0 \rangle \approx 0.6$. Solid lines are fits to a two-stage cascade model with $\tau_a = \tau_b = 0.53$ ps (see text for details). Inset: Absorption spectrum with probe wavelengths indicated. (b) Schematic of three-level system. π is a state in higher manifold; σ_2 is an intermediate state in the lowest manifold; and σ_1 is the lowest exciton state.

multistep process, consistent with the energy spectrum of 1D structures. The strong confinement in the transverse direction produces manifolds of 1D exciton states (see Figure 5b). The initial component corresponds to the relaxation of excitons from the initial excited exciton state to the ground exciton manifold. The later component comes from the relaxation within this dense energy manifold. Relaxation within the ground exciton manifold was studied in CdSe NRs.[11]

To quantify the energy relaxation, we introduce an approximate three-level model, with a high-energy state (π) that corresponds to the photoexcited exciton; an intermediate state (σ_2) in the lowest manifold of states; and the lowest exciton state (σ_1). Here π and σ_2 should be considered as groups of closely spaced states. The energy difference between σ_1 and σ_2 is taken to be the energy difference between the probe wavelengths of 1300 and 1414 nm, 70 meV. The relaxation sequence is $\pi \xrightarrow{\tau_b} \sigma_2 \xrightarrow{\tau_a} \sigma_1$. Due to inhomogeneous broadening, the transient-absorption signal will have contributions from both σ_1 and σ_2, but σ_2 will contribute more on the high-energy side, while σ_1 will contribute more on the low-energy side. The temporal instrument response was assumed to be a Gaussian with duration of 220 fs and incorporated in the fitting procedure. The best-fit traces are shown in Figure 2 as the solid lines. The best fit is obtained with τ_a and τ_b equal to 0.53 ps.

Admittedly, this model is crude and neglects detailed description of the dynamics between states in the same manifold. Due to limited signal-to-noise ratio, it is very hard to distinguish multiple components. Nevertheless, this model still provides useful information. The fact that τ_a and τ_b are similar means that the corresponding energy relaxation rates are very different. $\tau_b = 0.53$ ps implies an exciton energy relaxation rate of 1.1 eV/ps. If the electron and hole relax independently, the energy relaxation rate for each carrier would be 0.6 eV/ps. For comparison, the energy relaxation rate for the electron ranges from 0.15 to 1.0 eV/ps for PbSe quantum dots with diameters between 3.0 and 5.0 nm.[27] The comparable rates suggest that when carriers are in the high-energy manifold, they cool in the same way as in quantum dots: the electron and hole cool independently and they are not tightly bound. On the other hand, $\tau_a = 0.53$ ps implies an energy relaxation rate about 0.13 eV/ps. The reduced rate could be due to reduced density of possible final states as carriers relax to the band edge. In addition, the electrons and holes are more likely to be bound into excitons when they are sufficiently cold. Interaction between excitons and polar optical phonons is weak,[28,29] and this would further reduce the cooling rate.

Finally, we find that the initial stage of relaxation depends on excitation fluence. Figure 6 plots the rising edge with different pump fluence, at different probe wavelengths. The traces are normalized to their values at 3 ps to highlight the initial relaxation. Traces with different pump fluence overlap very well from 3 to 6 ps,

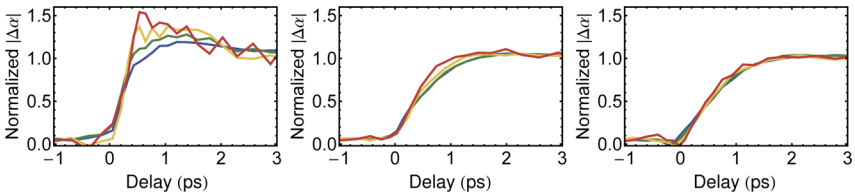

Figure 6. Normalized rising edge at different probe wavelength (1350, 1414, 1470 nm), with different pump fluence, corresponding to $\langle N \rangle$ = 3.3 (blue), 2.8 (green), 1.4 (yellow), and 0.8 (red). The traces are normalized to their values at long time (3 ps) for comparison.

which shows that the effect of Auger recombination due to different numbers of excitons is not present on this time scale. The rise in the ground-exciton population is faster at lower excitation levels. The trend is weaker on the low-energy side of the transition and stronger on the high-energy side of the transition. These measurements suggest that multiexciton states cool slower than single-exciton states. However, other explanations, such as hot-exciton-induced Stark effect, could yield similar results.[30,31] A more detailed understanding of exciton interaction is needed here to give a definite explanation.

DISCUSSION

We find that Auger relaxation is 3 to 4 times slower in NRs compared to quantum dots with the same energy gap. This is very roughly as expected due to the increased volume and, thus, reduced exciton density. Rupasov predicted theoretically that Auger recombination for the ground biexciton state is forbidden and, therefore, should be strongly suppressed,[20] which is clearly not observed here. Our results also differ from those of Cunningham *et al.*, who found that nanorods and quantum dots have similar biexciton lifetime.[21] The structures they studied were quasi-1D hyperbranched structures, which could be a reason for the discrepancy. A reduced Auger rate should be beneficial in applications to lasing. This has been demonstrated with CdSe nanostructures.[13,32] The energy-loss rate of single excited excitons in PbSe NRs is comparable to the rate in quantum dots. For MEG to be efficient, the energy relaxation of single excitons should be slower than the Coulomb scattering between single and multiexciton states.[29] Our observation of slower Auger relaxation in nanorods (for similar values of photon energy in units of the energy gap) and similar energy-loss rate would predict a lower MEG rate in NRs. We suggest that the apparent asymmetry between Auger recombination and MEG is a consequence of the densities of states. In Auger recombination, the biexciton density of states is not relevant because the biexciton is the initial state. In MEG, the biexciton density of states is a crucial factor, regardless of the precise mechanism. For impact ionization,[33] the number of final states increases, while with coherent coupling of single and multiexciton states,[29,31,34] the decoherence of multiexciton states becomes quicker. Considering the exciton moving in 1D, the total number of exciton states is proportional to the length of the NR. The density of states for the biexciton (if we neglect their interaction) would be a convolution of two single-exciton densities of states and, therefore, proportional to the square of length, much faster than the rise for single exciton states. This argument does not necessarily mean that the longer the wire, the higher the MEG efficiency. Momentum conservation, especially at high energy, would also limit the effective number of states that actually undergo MEG. More studies are needed to find the optimum size and dimensionality that would result in the highest MEG efficiency.

CONCLUSION

We described measurements of Auger relaxation of multiple excitons and intraband energy relaxation of charge carriers in PbSe nanorods. The biexciton lifetime of a nanorod is about the same as that of a quantum dot of the same volume, but is much larger than that of a quantum dot with the same energy gap. The multiexciton lifetimes scale approximately as expected for tightly bound excitons, which are expected in these 1D structures. The intraband energy relaxation of excited excitons proceeds in two stages: the 1Π to 1Σ relaxation has a 500 fs time constant, and this is followed by additional slower energy relaxation within the manifold of 1Σ states. These results will be important to future applications of lead-salt nanorods in light emitters and photovoltaics, among others.

METHODS

Chemicals. Selenium pellets (Aldrich, <5 mm, 99.999%), tris(diethylamino)phosphine (TDP, Aldrich, 97%), lead(II) oxide (PbO, Aldrich, 99.9%), oleic acid (OA, Aldrich, 90%), and 1-octadecene (ODE, Aldrich, 90%) were used.

PbSe NR Synthesis. The synthesis follows the procedure in Koh *et al.*'s paper.[16] The selenium precursor is prepared by dissolving selenium pellets (0.79 g, 10 mmol) into TDP (10 mL) overnight, forming a 1 M solution of TDPSe. The synthesis is performed using a standard Schlenk line. PbO (0.22 g, 1 mmol), OA (1 mL, ~3 mmol), and ODE (5 mL) are added to the reaction flask. The solution is vacuumed at <200 mTorr followed by N_2 gas under rapid stirring. This process is repeated three times before the solution is heated to 110 °C. The solution is again vacuumed for 3 min twice to get rid of water produced in the reaction. The solution is then heated to the desired injection temperature (170 °C in a typical synthesis) and allowed to stabilize. The 1 M TDPSe solution (3 mL, 3 mmol of Se) prepared

prior to the synthesis is obtained from the glovebox and quickly injected into the reaction flask. Upon injection, the temperature of the solution drops 10−20 °C below the injection temperature. The heating element is manually adjusted to keep the solution at a near constant temperature for a desired reaction time (3−5 min). Over the course of the reaction it is typical for the temperature to fluctuate within a 5 °C range. After the reaction, the flask is quickly placed in an ice bath while being stirred until the solution temperature reaches room temperature. A 5 mL portion of hexane is then injected into the solution. The solution is preciptated by acetone and ethanol. The precipitated nanorod is isolated by centrifugation at 2500 rpm for 5 min, redissolved in toluene, and placed into the glovebox.

Sample Preparation. Samples were prepared by suspending PbSe NRs in tetrachloroethylene. The samples were sealed in an air-free environment and removed just before the optical experiments. A 3 mm × 3 mm cuvette was used, with the concentration chosen to keep the optical density less than 0.3 at the excitation wavelengths. Experiments were performed with both static and flowing samples, and nearly identical results were obtained. Results presented were obtained without flowing the sample, which yielded better signal-to-noise ratios.

Transient Absorption Measurment. Standard transient saturated-absorption measurements on interband transitions were performed using a Ti:sapphire amplifier and optical parametric amplifier, which supply 130 fs pulses at 1 kHz repetition rate. The time resolution of the setup is 220 fs, determined by the cross-correlation of the 800 nm pump and ∼1500 nm probe pulses.

Conflict of Interest: The authors declare no competing financial interest.

Acknowledgment. This material is based upon work supported by the National Science Foundation under Grant No. EEC-0646547. This work made use of the electron microscopy and optical spectroscopy facilities of the Cornell Center for Materials Research (CCMR) with support from the National Science Foundation Materials Research Science and Engineering Centers (MRSEC) program (DMR 1120296). We thank A. Bartnik for help at the beginning of this work, W.-K. Koh and C. Murray for guidance on the synthesis of the nanorods, and J. Choi and D. Stachnik for suggestions on the manuscript.

Supporting Information Available: TEM images of all NR samples. Ensemble absorption spectra of all NR samples. Modeling of the effect of optical density. This material is available free of charge via the Internet at http://pubs.acs.org.

REFERENCES AND NOTES

1. Tang, J.; Kemp, K.; Hoogland, S.; Jeong, K.; Levina, L.; Furukawa, M.; Wang, X.; Debnath, R.; Cha, D.; Chou, K.; Fischer, A.; Amassian, A.; Asbury, J. B.; Sargent, E. H. Colloidal-Quantum-Dot Photovoltaics Using Atomic-Ligand Passivation. *Nat. Mater.* **2011**, *10*, 765–771.
2. Li, Y.; Qian, F.; Xiang, J.; Lieber, C. Nanowire Electronic and Optoelectronic Devices. *Mater. Today* **2006**, *9*, 18–27.
3. Kuno, M. An Overview of Solution-Based Semiconductor Nanowires: Synthesis and Optical Studies. *Phys. Chem. Chem. Phys.* **2008**, *10*, 620.
4. Krahne, R.; Morello, G.; Figuerola, A.; George, C.; Deka, S.; Manna, L. Physical Properties of Elongated Inorganic Nanoparticles. *Phys. Rep.* **2011**, *501*, 75–221.
5. Chepic, D.; Efros, A.; Ekimov, a.I.; Ivanov, M.; Kharchenko, V.; Kudriavtsev, I.; Yazeva, T. Auger Ionization of Semiconductor Quantum Drops in a Glass Matrix. *J. Lumin.* **1990**, *47*, 113–127.
6. Klimov, V. I. Spectral and Dynamical Properties of Multiexcitons in Semiconductor Nanocrystals. *Annu. Rev. Phys. Chem.* **2007**, *58*, 635–73.
7. Klimov, V. I. Optical Gain and Stimulated Emission in Nanocrystal Quantum Dots. *Science* **2000**, *290*, 314–317.
8. Schaller, R.; Petruska, M.; Klimov, V. Tunable Near-Infrared Optical Gain and Amplified Spontaneous Emission Using PbSe Nanocrystals. *J. Phys. Chem. B* **2003**, *107*, 13765–13768.
9. Schaller, R.; Klimov, V. High Efficiency Carrier Multiplication in PbSe Nanocrystals: Implications for Solar Energy Conversion. *Phys. Rev. Lett.* **2004**, *92*, 186601.
10. Mohamed, M. B.; Burda, C.; El-Sayed, M. A. Shape Dependent Ultrafast Relaxation Dynamics of CdSe Nanocrystals: Nanorods *vs* Nanodots. *Nano Lett.* **2001**, *1*, 589–593.
11. Achermann, M.; Bartko, A. P.; Hollingsworth, J. A.; Klimov, V. I. The Effect of Auger Heating on Intraband Carrier Relaxation in Semiconductor Quantum Rods. *Nat. Phys.* **2006**, *2*, 557–561.
12. Yu, P.; Nedeljkovic, J. M.; Ahrenkiel, P. A.; Ellingson, R. J.; Nozik, A. J. Size Dependent Femtosecond Electron Cooling Dynamics in CdSe Quantum Rods. *Nano Lett.* **2004**, *4*, 1089–1092.
13. Htoon, H.; Hollingsworth, J.; Dickerson, R.; Klimov, V. Effect of Zero- to One-Dimensional Transformation on Multiparticle Auger Recombination in Semiconductor Quantum Rods. *Phys. Rev. Lett.* **2003**, *91*, 227401.
14. Huang, L.; Krauss, T. Quantized Bimolecular Auger Recombination of Excitons in Single-Walled Carbon Nanotubes. *Phys. Rev. Lett.* **2006**, *96*, 057407.
15. Klimov, V.; McGuire, J.; Schaller, R.; Rupasov, V. Scaling of Multiexciton Lifetimes in Semiconductor Nanocrystals. *Phys. Rev. B* **2008**, *77*, 195324.
16. Koh, W.-K.; Bartnik, A. C.; Wise, F. W.; Murray, C. B. Synthesis of Monodisperse PbSe Nanorods: A Case for Oriented Attachment. *J. Am. Chem. Soc.* **2010**, *132*, 3909–13.
17. Bartnik, A.; Efros, A.; Koh, W.-K.; Murray, C.; Wise, F. Electronic States and Optical Properties of PbSe Nanorods and Nanowires. *Phys. Rev. B* **2010**, *82*, 195313.
18. Rupasov, V. Electronic Structure and Optical Properties of Quantum-Confined Lead Salt Nanowires. *Phys. Rev. B* **2009**, *80*, 115306.
19. Kang, I.; Wise, F. W. Electronic Structure and Optical Properties of PbS and PbSe Quantum Dots. *J. Opt. Soc. Am. B* **1997**, *14*, 1632.
20. Rupasov, V. I. Temperature and Size-Dependent Suppression of Auger Recombination in Quantum-Confined Lead-Salt Nanowires. *Phys. Rev. B* **2010**, *81*, 041313(R).
21. Cunningham, P. D.; Boercker, J. E.; Foos, E. E.; Lumb, M. P.; Smith, A. R.; Tischler, J. G.; Melinger, J. S. Enhanced Multiple Exciton Generation in Quasi-One-Dimensional Semiconductors. *Nano Lett.* **2011**, *11*, 3476–81.
22. Klimov, V. Optical Nonlinearities and Ultrafast Carrier Dynamics in Semiconductor Nanocrystals. *J. Phys. Chem. B* **2000**, *104*, 6112–6123.
23. Wehrenberg, B.; Wang, C.; Guyot-Sionnest, P. Interband and Intraband Optical Studies of PbSe Colloidal Quantum Dots. *J. Phys. Chem. B* **2002**, *106*, 10634–10640.
24. Harbold, J.; Du, H.; Krauss, T.; Cho, K.; Murray, C. Time-Resolved Intraband Relaxation of Strongly Confined Electrons and Holes in Colloidal PbSe Nanocrystals. *Phys. Rev. B* **2005**, *72*, 195312.
25. Moreels, I.; Lambert, K.; De Muynck, D.; Vanhaecke, F.; Poelman, D.; Martins, J. C.; Allan, G.; Hens, Z. Composition and Size-Dependent Extinction Coefficient of Colloidal PbSe Quantum Dots. *Chem. Mater.* **2007**, *19*, 6101–6106.
26. Robel, I.; Gresback, R.; Kortshagen, U.; Schaller, R.; Klimov, V. Universal Size-Dependent Trend in Auger Recombination in Direct-Gap and Indirect-Gap Semiconductor Nanocrystals. *Phys. Rev. Lett.* **2009**, *102*, 177404.
27. Schaller, R. D.; Pietryga, J. M.; Goupalov, S. V.; Petruska, M. A.; Ivanov, S. A.; Klimov, V. I. Breaking the Phonon Bottleneck in Semiconductor Nanocrystals *via* Multiphonon Emission Induced by Intrinsic Nonadiabatic Interactions. *Phys. Rev. Lett.* **2005**, *95*, 196401.
28. Schmitt-Rink, S.; Miller, D. Theory of the Linear and Nonlinear Optical Properties of Semiconductor Microcrystallites. *Phys. Rev. B* **1987**, *35*, 8113–8125.
29. Shabaev, A.; Efros, A. L.; Nozik, A. J. Multiexciton Generation by a Single Photon in Nanocrystals. *Nano Lett.* **2006**, *6*, 2856–63.

30. Ji, M.; Park, S.; Connor, S. T.; Mokari, T.; Cui, Y.; Gaffney, K. J. Efficient Multiple Exciton Generation Observed in Colloidal PbSe Quantum Dots with Temporally and Spectrally Resolved Intraband Excitation. *Nano Lett.* **2009**, *9*, 1217–22.
31. Ellingson, R. J.; Beard, M. C.; Johnson, J. C.; Yu, P.; Micic, O. I.; Nozik, A. J.; Shabaev, A.; Efros, A. L. Highly Efficient Multiple Exciton Generation in Colloidal PbSe and PbS Quantum Dots. *Nano Lett.* **2005**, *5*, 865–71.
32. Kazes, M.; Lewis, D.; Ebenstein, Y.; Mokari, T.; Banin, U. Lasing from Semiconductor Quantum Rods in a Cylindrical Microcavity. *Adv. Mater.* **2002**, *14*, 317–321.
33. Allan, G.; Delerue, C. Role of Impact Ionization in Multiple Exciton Generation in PbSe Nanocrystals. *Phys. Rev. B* **2006**, *73*, 205423.
34. Witzel, W.; Shabaev, A.; Hellberg, C.; Jacobs, V.; Efros, A. Quantum Simulation of Multiple-Exciton Generation in a Nanocrystal by a Single Photon. *Phys. Rev. Lett.* **2010**, *105*, 137401.